THE JOURNAL OF BIOLOGICAL CHEMISTRY VOL. 290, NO. 49, pp. 29402–29413, December 4, 2015

Macrophage-specific *de Novo* Synthesis of Ceramide Is Dispensable for Inflammasome-driven Inflammation and Insulin Resistance in Obesity*

Received for publication, July 21, 2015, and in revised form, September 18, 2015 Published, JBC Papers in Press, October 5, 2015, DOI 10.1074/jbc.M115.680199

Christina D. Camell[‡§], Kim Y. Nguyen[‡§], Michael J. Jurczak[¶], Brooke E. Christian[‖], Gerald I. Shulman[¶], Gerald S. Shadel[¶], and Vishwa Deep Dixit[‡§1]**

*From the [‡]Section of Comparative Medicine and [§]Department of Immunobiology, Departments of [¶]Internal Medicine, [‖]Pathology, and **Genetics, Yale School of Medicine, New Haven, Connectitcut 06520*

Dietary lipid overload and calorie excess during obesity is a low grade chronic inflammatory state with diminished ability to appropriately metabolize glucose or lipids. Macrophages are critical in maintaining adipose tissue homeostasis, in part by regulating lipid metabolism, energy homeostasis, and tissue remodeling. During high fat diet-induced obesity, macrophages are activated by lipid derived "danger signals" such as ceramides and palmitate and promote the adipose tissue inflammation in an Nlrp3 inflammasome-dependent manner. Given that the metabolic fate of fatty acids in macrophages is not entirely elucidated, we have hypothesized that *de novo* synthesis of ceramide, through the rate-limiting enzyme serine palmitoyltransferase long chain (Sptlc)-2, is required for saturated fatty acid-driven Nlrp3 inflammasome activation in macrophages. Here we report that mitochondrial targeted overexpression of catalase, which is established to mitigate oxidative stress, controls ceramide-induced Nlrp3 inflammasome activation but does not affect the ATP-mediated caspase-1 cleavage. Surprisingly, myeloid cell-specific deletion of *Sptlc2* is not required for palmitate-driven Nlrp3 inflammasome activation. Furthermore, the ablation of *Sptlc2* in macrophages did not impact macrophage polarization or obesity-induced adipose tissue leukocytosis. Consistent with these data, investigation of insulin resistance using hyperinsulinemic-euglycemic clamps revealed no significant differences in obese mice lacking ceramide *de novo* synthesis machinery in macrophages. These data suggest that alternate metabolic pathways control fatty acid-derived ceramide synthesis in macrophage and the Nlrp3 inflammasome activation in obesity.

Diet-induced obesity (DIO)[2] is a growing epidemic and has greatly augmented the number of humans diagnosed with metabolic diseases such as type 2 diabetes, cardiovascular disease, and atherosclerosis (1, 2). The importance of inflammation in driving metabolic dysregulation during DIO is well established, and research has highlighted the importance of the adipose tissue and resident immune cells in maintaining glucose homeostasis (3, 4).

DIO induces adipose tissue inflammation that is largely characterized by infiltration of immune cells, including pro-inflammatory activated macrophages, T cells, and B cells (5–8). In lean adipose, resident macrophages exhibit anti-inflammatory characteristics, including expressing surface markers such as MGL1, CD206, and Arginase1. In contrast, infiltrating macrophages express increased amounts of inflammatory cytokines, such as TNFα, MCP1, and IL1β (7). Infiltrating CCR2$^+$ macrophages surround dying adipocytes, forming crown-like structures, and contain large lipid droplets (9, 10), suggesting they are uniquely sensitive to the lipid-loaded microenvironment. Diet-induced inflammation is mediated through the activation of the NLRP3 (NLR family pyrin domain containing 3) inflammasome, a large cytosolic multiprotein scaffolding complex that activates caspase-1 and leads to the secretion of bioactive IL1β (11, 12). Inflammasome activation has been shown to impair insulin sensitivity in adipose tissue, liver, and skeletal muscle and increases adipose tissue inflammation (13–16).

In humans and mouse models, DIO is also characterized by alterations in lipid metabolism, excess lipid availability, and increased ceramides systemically and in the adipose tissue (17–19). In lipid metabolism, the fatty acid oxidative pathway utilizes palmitoyl-CoA to fuel mitochondrial oxidative phosphorylation; alternatively palmitate enters the nonoxidative pathway to be converted into ceramide via irreversible condensation with L-serine by the rate-limiting enzyme serine palmitoyltransferase (SPT) (20). SPT is a heterodimer, is present in the endoplasmic reticulum, and is composed of mainly two subunits, Sptlc1 and Sptlc2 (20). Ceramides and other sphingolipids are structural components of membranes and signaling molecules, which serve to mediate cell homeostasis (20); however, dysregulated increase in ceramide content in cells is linked to elevated inflammation and insulin resistance (21, 22). Inhibition of ceramide synthesis prevents lipid-induced insulin resistance, diet-induced insulin resistance, and hepatic steatosis (23–25)

In addition to up-regulating ceramide synthesis, palmitate treatment of macrophages inhibits AMPK activation, generates

* This work was supported by National Institutes of Health Grants DK090556, AG043608, and AI105097 (to V. D. D.); AG047632 (to G. S. S.); NRSA NS077723 (to B. E. C.); DK-40936, DK-059635, and DK-45735 (to G. I. S.); and AG043608 (to C. D. C.). The authors declare that they have no conflicts of interest with the contents of this article. The content is solely the responsibility of the authors and does not necessarily represent the official views of the National Institutes of Health.

[1] To whom correspondence should be addressed: Section of Comparative Medicine and Dept. of Immunobiology, Yale School of Medicine, 310 Cedar St., New Haven CT 06520. Tel.: 203-785-2525; Fax: 203-785-7499; E-mail: Vishwa.Dixit@yale.edu.

[2] The abbreviations used are: DIO, diet-induced obesity; SPT, serine palmitoyltransferase; ROS, reactive oxygen species; LFD, low fat diet; HFD, high fat diet; BMDM, bone marrow-derived macrophage; MCAT, membrane-targeted catalase.

TABLE 1
Sequences of primers used in Syber green quantitative PCR
Forward and reverse sequences are listed (5′ to 3′) for *Gapdh*, *Arg1*, *Tnfα*, *Il1β*, *iNos*, *Sptlc1*, *Sptlc2*, *Sptlc3*, *CerS5*, *CerS6*, *Nsmaf*, and *Smpd1*.

Gene	Forward	Reverse
Gapdh	TCAACGGCACAGTCAAG	CATGGACTGTGGTCATGAG
Arg1	ATTATCGGAGCGCCTTTCTC	TTTTTCCAGCAGACCAGCTT
Tnfα	CGAGTGACAAGCCTGTAGC	CTTTCTCCTGGTATGAGATAGCA
Il1β	GGTCAAAGGTTTGGAAGCAG	TGTGAAATGCCACCTTTTGA
iNos	CCCTCCTGATCTTGTGTTGG	GGCAGTGCATACCACTTCAA
Sptlc1	AGTCACCGAGCACTATGGGA	GAGAGCCGCTGATGGTCAA
Sptlc2	CCAAAATTGGCGCCTTTGGA	GGGTAGCAGGAAATCCCACC
Sptlc3	GACTAGTAAAAGGCTCTGCCCT	ATTGGTCGGATGTGCTGGAG
CerS5	ATCAGGACAAGCCTCCAACG	AACCAAGGCATCGACCAGAG
CerS6	AGGGTTGAACTGCTTCTGGTC	GTCATCCTTGGATACCTTGCCT
Nsmaf	TGAACATGATGTCAGCGTCAA	CACCATGCCTTCTTTGGTGC
Smpd1	GACCACTAGCTGTAGCCTTCC	AACTCGGTAGCCAGGGTTAAG

reactive oxygen species, and activates the NLRP3 inflammasome causing the secretion of IL1β (15, 26). The role for the nonoxidative lipid metabolism pathway in regulating NLRP3 inflammasome is not clear; given the association of mitochondrial oxidative stress with cellular lipid accumulation, we have hypothesized that *de novo* synthesis of ceramide via *Sptlc2* is required for inflammasome-induced inflammation in diet-induced obesity. We found that ceramide-induced IL1β requires Nlrp3 and the accumulation of reactive oxygen species (ROS); however, surprisingly, we found that palmitate-induced IL1β does not require *Sptlc2*, indicating that *Sptlc2* is not necessary for Nlrp3 inflammasome activation. Furthermore, we show that saturated fat diet-induced adipose tissue inflammation is unaffected in isolated adipose tissue macrophages from mice with myeloid cell deletion of *Sptlc2*. Our findings reveal that *in vitro* and *in vivo*, myeloid cell-specific *Sptlc2* is dispensable for fatty acid-mediated inflammation and insulin resistance.

Materials and Methods

Animals/Mice—Sptlc2-flox mice have been previously described (27). To ablate *de novo* synthesis in myeloid cells, *Sptlc2*-flox (*Sptlc2*$^{fl/fl}$; Dr. Xian-Cheng Jiang, SUNY) mice were crossed to LysM-Cre (B6.129P2-*Lyz2*$^{tm1(cre)Ifo}$/J; Jackson Laboratory) mice to generate *Sptlc2*$^{fl/-}$ LysM$^{cre/-}$ mice. *Sptlc2*$^{fl/-}$ LysM$^{cre/-}$ mice were backcrossed to *Sptlc2*$^{fl/fl}$ mice generating the littermates *Sptlc2*$^{fl/fl}$ LysM$^{-/-}$ (CRE^{-}) controls and Sptlc2$^{fl/fl}$ LysM$^{cre/-}$ (CRE^{+}) experimental animals. MCAT transgenic mice and wild-type littermate controls were obtained from Dr. Gerald Shadel (Yale University) and have been previously described (28). For diet studies, mice were placed on a standard chow diet (LFD; 13.4% fat; LabDiet, Purina 5001) or a high fat diet (HFD; 60% fat; Research Diets) at 6–7 weeks of age for 13 weeks of feeding. All experiments and animal use were conducted in compliance with the National Institute of Health Guide for the Care and Use of Laboratory Animals and were approved by the Institutional Animal Care and Use Committee at Yale University.

Bone Marrow-derived Macrophage (BMDMs) and Cell Culture—The BMDMs were prepared, and inflammasome activation assays were performed as described by us previously (13, 32). All steps were performed using sterile technique. Femurs were collected in RPMI (Life Technologies, Inc.). Using a needle and syringe, marrow was flushed into RPMI containing 10% FBS (Omega Scientific, Inc.) and 5% antibacterial/antimycotics (Life Technologies, Inc.). Red blood cells were lysed using ammonium-chloride-potassium lysis buffer (Quality Biological), and lysis was neutralized with RPMI. Bone marrow cells were differentiated into macrophages using MCSF (10 ng/ml; R&D) and L929 conditioned medium. Nonadherent cells were collected on day 7, counted, and replated at 1 × 10^6 cells/ml. BMDMs were treated on day 8. Cells were primed by 4 h of treatment with ultrapure LPS (1 μg/ml; Sigma) alone; inflammasome stimulation was provided by treatment with ATP (5 mM; 1 h), sodium palmitate conjugated to BSA (200 or 400 μM; 24 h of treatment; Sigma) or ceramide (40–120 mg; 6 h; Cayman Chemical). Myriocin (Caymen Chemical) was added to some treatments, in combination with LPS priming, at 1 or 5 μM. Supernatants were collected and stored at −80 °C. BMDMs were washed with PBS and collected in radioimmune precipitation assay buffer supplemented with protease inhibitors for protein analysis. BMDMs were polarized to M1 or M2 by treatment with LPS (1 μg/ml) and IFNγ (20 ng/ml; eBioscience) or IL4 (10 ng/ml; eBioscience). After 24 h, cells were washed with PBS and collected in TRIzol for RNA extraction.

Western Blot—Samples were left on ice for 1 h with vortexing every 10 min to disrupt membranes. Samples were centrifuged at 14,000 × *g* for 15 min, supernatant was collected, and protein concentration was quantified using the DC protein assay (Bio-Rad). We probed for IL1β (GeneTex), SPTLC2 (Proteintech), catalase (Sigma), caspase-1 (Genentech), and actin (Cell Signaling).

RNA Extraction and Gene Expression Analysis—RNA extraction and purification were performed using RNeasy kits (Qiagen) according to the manufacturer's instructions. Total RNA was measured using a nanodrop and 500 ng used to reverse transcribe cDNA. Quantitative PCR was performed as described (29). Primer sequences for *Gapdh*, *Arg1*, *Tnfα*, *Il1β*, *iNos*, *Sptlc1*, *Sptlc2*, *Sptlc3*, *CerS5*, *CerS6*, *Nsmaf*, and *Smpd1* are listed in Table 1.

Adipose Digestion and Stromavascular Staining—Visceral adipose was harvested at sacrifice and weighed. Tissue was enzymatically digested in 0.1% collagenase I (Worthington Biochemicals) in Hanks' buffered salt solution (Life Technologies, Inc.) for 45 min at 37 °C. The stromavascular fraction was pelleted by centrifugation at 1500 rpm for 10 min, then washed, and filtered. Red blood cells are lysed using ACK lysing buffer. Cells were resuspended in 1 ml for counting prior to staining or

positive selection of F4/80$^+$ macrophages (Biotinylated; eBioscience) using Dynabeads biotine binder (Life Technologies, Inc.). Positively selected cells were stored in TRIzol for RNA isolation. For staining, the stromavascular fraction was incubated with FcBlock and surface antibodies for 30 min on ice in the dark, then washed, and stained with fixable viability dye (eBioscience) and intracellular antibodies using Cytofix (BD Bioscience). Analysis was performed on a BD LSRII and using FlowJo vX.

Antibodies—The following antibodies were used: fixable viability dye aqua; F4/80-eFlour450; CD11b-PerCPCy5.5; CD11c-APC; CD206-PECCy7; CD3-FITC; B220-PECy7; and MHCII-Alexa Fluor 700 (eBioscience).

Hyperinsulinemic-Euglycemic Clamps—Experiments were performed according to recent recommendations of the Mouse Metabolic Phenotyping Center Consortium (30) and as previously published (31).

Glucose and Insulin Tolerance Test—Mice were fasted for 12 h (glucose tolerance test) or 4 h (insulin tolerance test), and blood glucose was measured from the tail vein using a glucometer (Breeze) at baseline, 10, 20, 30, 45, 60, and 90 min. Insulin (Sigma-Aldrich) was injected intraperitoneally at 0.8 unit/kg. Glucose (Sigma-Aldrich) was injected intraperitoneally at 0.4 g/kg.

Statistical Analysis—We used a two-tailed Student's *t* test to determine the significance between genotypes. The differences between means and the effects of treatments were analyzed by one-way analysis of variance with Tukey's test which corrects for multiple hypotheses.

Results

Ceramides Activate the Nlrp3 Inflammasome via Mitochondrial Oxidative Stress—Our prior studies have demonstrated that ceramides activate caspase-1-induced IL1β secretion in a Nlrp3 inflammasome-dependent manner (13, 32); however, the exact mechanism by which ceramides activate the Nlrp3 inflammasome is not yet understood. Consistent with our previous studies, ceramide activates Nlrp3 inflammasome, causing IL1β secretion from BMDMs in a dose-dependent manner (Fig. 1, *A* and *B*). Given that ceramides and lipids increase the production of ROS causing oxidative stress and that mitochondrial damage and ROS generation has been linked to the activation of the Nlrp3 inflammasome (33, 34), we tested the potential role of ROS in ceramide-induced inflammasome activation. We investigated this question using BMDMs from transgenic mice with targeted overexpression of the human catalase gene to mitochondria (MCAT mice), an enzyme that reduces mitochondrial oxidative damage and improves mitochondrial function by degrading hydrogen peroxide and preventing ROS accumulation (35, 36). Consistent with recent studies (37) that ROS is not critical for ATP-mediated inflammasome activation, catalase overexpression did not attenuate extracellular ATP-induced caspase-1 activation (Fig. 1*C*). In contrast, ceramide-induced caspase-1 activation was decreased in BMDMs from MCAT transgenic mice, indicating that inhibition of ROS accumulation prevents ceramide-induced Nlrp3 activation (Fig. 1*C*), and similar to saturated fatty acids, ceramide induction of mitochondrial oxidative stress drives Nlrp3 activation.

Mitochondrial oxidative activity is associated with intracellular lipid accumulation (38, 39); we wanted to ask whether prevention of lipid accumulation could reduce ROS-induced Nlrp3 activation. SPT is the rate-limiting enzyme in the *de novo* synthesis of ceramide (Fig. 1*D*) and is an important intersection for regulating cellular levels of saturated fatty acids and sphingolipids by generating ceramide from palmitoyl-CoA precursors (20). SPT-specific inhibition, using myriocin, prevents palmitate-induced accumulation of ceramide and downstream cytokine production in macrophages (26). Palmitate induces IL1β secretion in a Nlrp3-dependent manner (Fig. 1*B* and Ref. 15); however, myriocin-inhibition of SPT failed to abrogate IL1β secretion (Fig. 1*E*). These data suggest that chemical inhibition of *de novo* synthesis may not be sufficient to reduce saturated fat-induced IL1β.

Myeloid Cell-specific Deletion of Serinepalmitoyltransferase 2—To further address the role of SPT in saturated fat-induced Nlrp3 activation, we wanted to genetically delete SPT; therefore we first measured the expression level of *Sptlc* subunits in BMDMs. *Sptlc2* has the highest expression level, being nearly 5-fold higher than *Sptlc1* in pro-inflammatory-polarized M1 macrophages and in anti-inflammatory-polarized M2 macrophages (Fig. 2*A*). *Sptlc3* was not detected in BMDMs under any condition (Fig. 2*A*).

We sought to generate mice with myeloid cell-specific knockouts of *Sptlc2.* To test for cre recombinase deletion efficiency, we compared gene expression between littermates *Sptlc2*$^{fl/fl}$ LysM$^{-/-}$ (CRE$^-$) controls and Sptlc2$^{fl/fl}$ LysM$^{cre/-}$ (CRE$^+$) experimental BMDMs. In both M1 and M2 polarized BMDMs, *Sptlc2* gene was significantly reduced in CRE$^+$ mice as compared with their CRE$^-$ littermate control (Fig. 2*B*). *Sptlc2* gene level was not affected by polarization toward M1 or M2 phenotype or by having a single allele floxed (fl/−; CRE$^+$). The expression level of *Sptlc1* was unaltered by genotype or macrophage polarization (Fig. 2*B*). The immunoblot analysis confirmed that compared with littermate control cells, Sptlc2 protein was not expressed in CRE$^+$ BMDMs (Fig. 2*C*). These data indicate that in BMDMs from CRE$^+$, *Sptlc2* is efficiently deleted, without altering the expression of *Sptlc1*.

Sptlc2-deficient BMDM Activation in Vitro—Sptlc2 heterozygous macrophages have reduced palmitate-induced inflammatory gene expression and myeloid cell-specific deletion of *Sptlc2* improves atherosclerotic lesions (40). To examine *in vitro* whether CRE$^+$ macrophages are appropriately activated by traditional pro- or anti-inflammatory cytokines, we analyzed gene expression of traditional M1 or M2 markers following polarization of BMDMs from CRE$^-$ or CRE$^+$ mice. M1 macrophages from CRE$^-$ or CRE$^+$ mice had comparable expression levels of the M1 markers *Tnfα* and *iNos* but failed to express the M2 marker, *Arg1* (Fig. 3*A*). Similarly, M2 polarized macrophages from CRE$^-$ and CRE$^+$ mice had comparable expression levels of *Arg1* (Fig. 3*A*) but failed to express *Tnfα* and *iNos*. These data indicate that *Sptlc2* deficiency in macrophages does not alter macrophage polarization toward M1 or M2.

To examine whether the *de novo* synthesis pathway is required for saturated fatty acid activation of the inflammasome, BMDMs from CRE$^-$ or CRE$^+$ mice were primed with LPS prior to overnight culture in palmitate to activate the

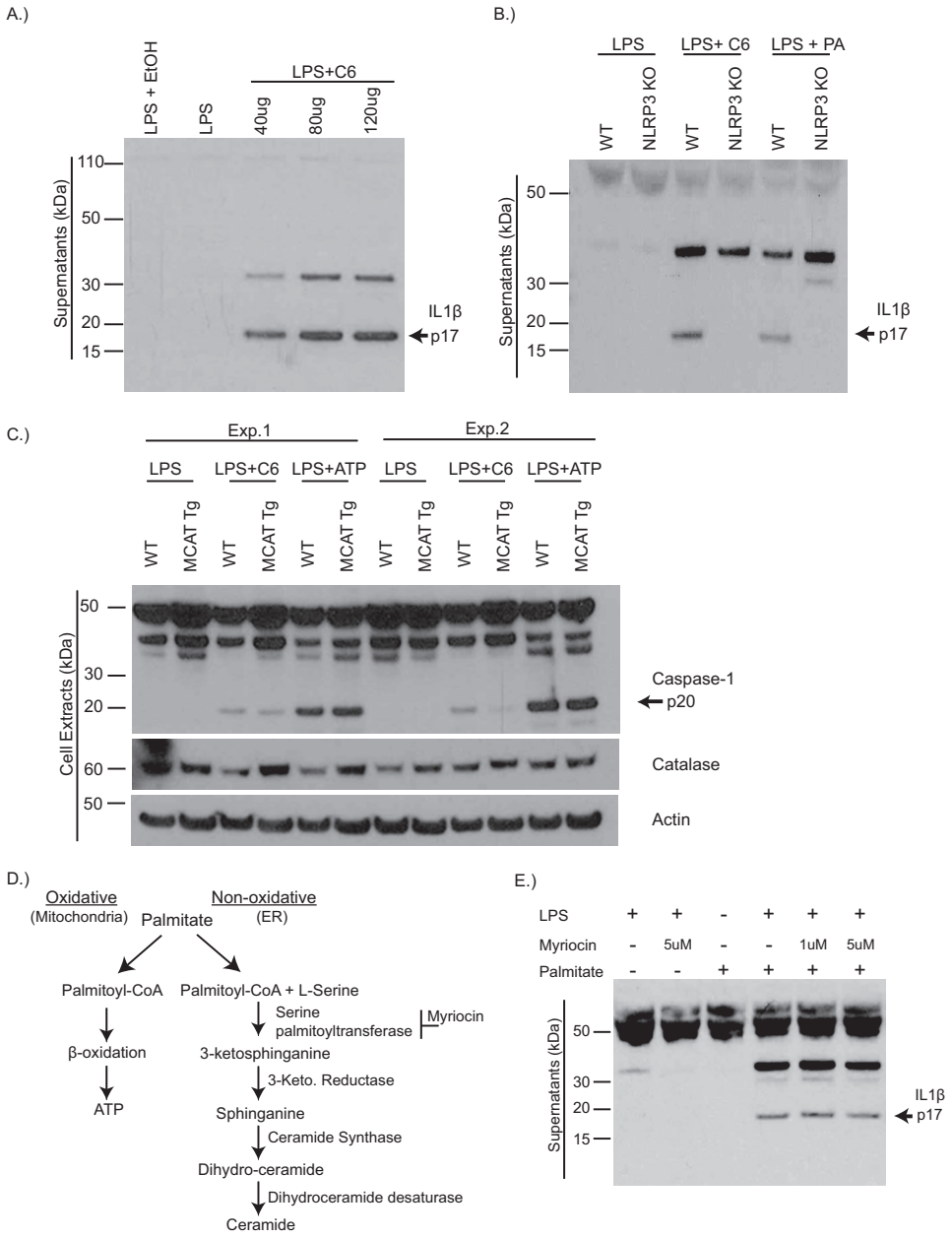

FIGURE 1. **Ceramides activate the Nlrp3 inflammasome via mitochondrial oxidative stress.** *A*, representative Western blot analysis of IL1β (active p17) protein in supernatants of WT BMDMs that have been primed with LPS for 4 h and stimulated with increasing doses of ceramide (C6) for 6 h. *B*, Western blot analysis of IL1β protein in BMDMs from WT or *Nlrp3*$^{-/-}$ mice that have been stimulated with LPS, LPS plus C6 (80 μg/ml) for 6 h, or LPS plus palmitate (400uM) for 24 h. *C*, Western blot analysis of caspase-1 (active p20) and catalase protein in BMDMs from WT or MCAT transgenic mice that have been treated with LPS alone, LPS plus C6, or LPS plus ATP (5 mM) for 1 h. Two representative blots from individual experiments are shown. *D*, schematic depicting palmitate entry into oxidative pathway to generate ATP or the nonoxidative pathway causing the *de novo* synthesis of ceramide. *E*, Western blot analysis of IL1β protein in the supernatants of WT BMDMs, treated with LPS or LPS plus palmitate, in which some received pretreatment with serine palmitoyltransferase inhibitor, myriocin. The data are representative of two or three individual experiments. *Exp.*, experiment.

inflammasome. Secretion of active IL1β into the supernatants was comparable between CRE$^-$ and CRE$^+$ BMDMs that were cultured with LPS plus palmitate (Fig. 3*B*). Surprisingly, secretion of active IL1β in the presence of ATP or ceramide was higher in BMDMs from CRE$^+$ mice, as compared with the CRE$^-$ BMDMs. These data indicate that Sptlc2 is not required for palmitate-induced Nlrp3 activation but may have role in inhibiting Nlrp3 activation, in the presence of other activators.

Macrophage SPTLC2 Deficiency Does Not Regulate Adipose Tissue Mass or Leukocytosis in Response to High Fat Diet—Saturated fat diet-induced obesity is characterized by increased adipose tissue mass and inflammation that involves increased numbers of macrophages surrounding hypertrophied adipocytes with increased ER stress and releases fatty acids upon cell death (3). Adipose tissue macrophage fatty acid uptake during obesity is a contributing factor of their inflammatory status (9); however, the fate of lipids in macrophages in still unclear. To identify whether myeloid cell-specific *de novo* synthesis of ceramides is required for adipose tissue inflammation driven by a high saturated fat diet, CRE$^-$ or CRE$^+$ mice were fed a 60% saturated fat diet for 13 weeks prior to analysis of the visceral adipose tissue. CRE$^-$ or CRE$^+$ mice on the HFD showed

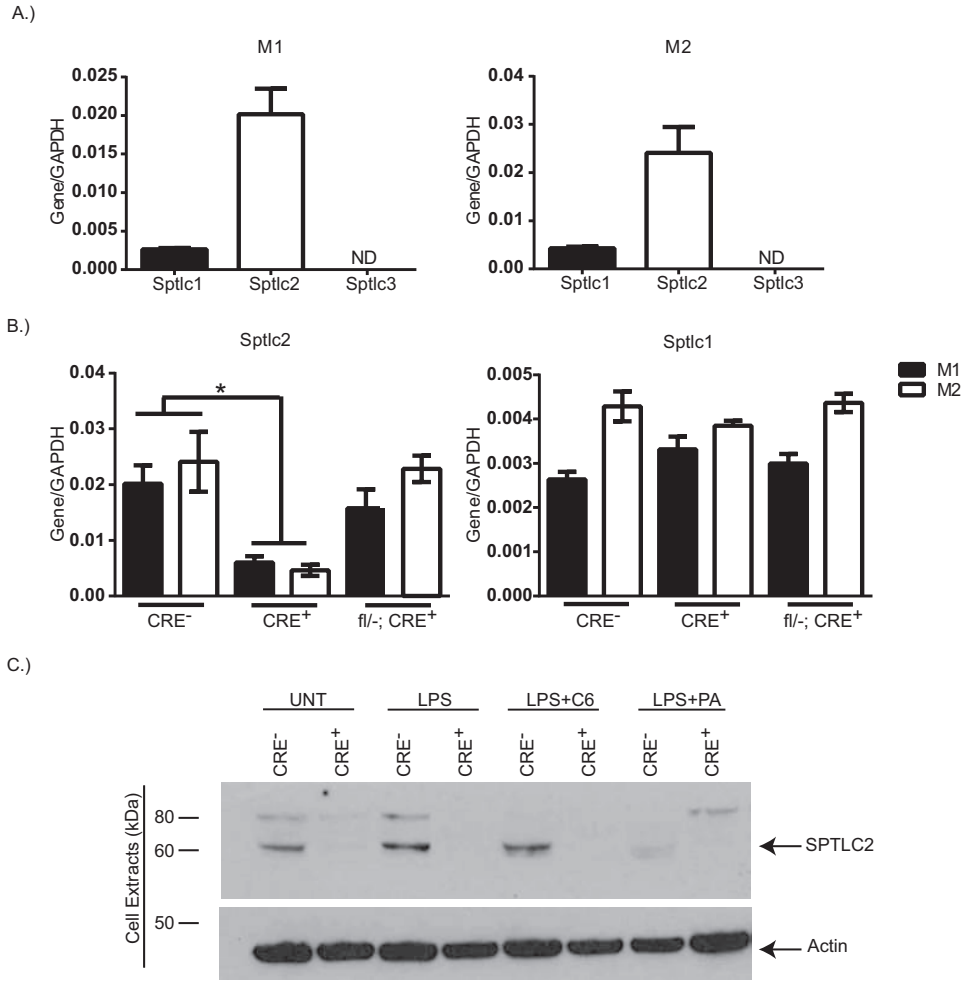

FIGURE 2. **Myeloid cell-specific deletion of *Sptlc2*.** *A*, gene expression of *Sptlc1*, *Sptlc2*, and *Sptlc3*, normalized to *gapdh*, in WT BMDMs that have been polarized to M1 (LPS (1 μg/ml) plus IFNγ (20 ng/ml)) or M2 (IL4 (10 ng/ml)). *B*, gene expression of *Sptlc2* or *Sptlc1* normalized to *gapdh* in M1 (*filled bars*) or M2 (*open bars*) polarized BMDMs from CRE$^-$, CRE$^+$, or fl/$-$; CRE$^+$. *C*, Western blot analysis of SPTLC2 protein expression in treated BMDMs from CRE$^-$ or CRE$^+$ mice. Actin is shown as a loading control (n = 2–3 individual experiments; t test). *, $p < 0.05$. The *error bars* represent means ± S.E.

increased weight gain (data not shown) and total body weight over control mice on a LFD, but there was no difference between CRE$^-$ and CRE$^+$ mice on HFD (Fig. 4*A*). Similarly, HFD-fed mice showed increased visceral adipose tissue mass and increased cellularity in visceral adipose tissue, but there were no differences between CRE$^-$ and CRE$^+$ mice (Fig. 4, *B* and *C*).

Adipose tissue macrophages play a major role in regulating the homeostasis of the adipose tissue (41). Pro-inflammatory macrophages are recruited to the adipose tissue during HFD, where they promote the inflammatory response by secreting inflammatory cytokines such as IL1β and TNFα (41). The gating strategy for quantifying adipose tissue macrophages and lymphocytes are shown in Fig. 4*D* with representative dot plots in Fig. 4*E*. Adipose tissue macrophages were characterized into M1 (CD11c$^+$), M2 (CD206$^+$), and HFD-induced CD11c$^+$CD206$^+$ macrophages. We found that the percentages of total F4/80$^+$ CD11b$^+$ macrophages are increased with HFD (Fig. 4*F*). When examining the subpopulation of macrophages, there was a small increase in the percentage of F4/80$^+$ CD11b$^+$CD11c$^+$CD206$^+$ macrophages that are increased in both CRE$^-$ and CRE$^+$ mice on HFD, as compared with control mice on LFD (Fig. 4*F*). Because lymphocyte populations are altered with HFD (5, 42), we quantified T and B cells in the visceral adipose tissue in HFD-fed mice. CD3$^+$ T cells and B220$^+$ B cells were comparable between CRE$^-$ and CRE$^+$ on HFD (Fig. 4*G*).

When normalized to the adipose tissue weight, the number of total F4/80$^+$ CD11b$^+$ macrophages and F4/80$^+$ CD11b$^+$ CD11c$^+$CD206$^+$ macrophages were significantly increased in both CRE$^-$ and CRE$^+$ on HFD as compared with control mice on LFD (Fig. 5*A*). To examine the gene expression of adipose tissue macrophages; F4/80$^+$ cells were positively selected from CRE$^-$ and CRE$^+$ mice on HFD. *Sptlc2* gene expression was significantly reduced in macrophages from CRE$^+$ mice, whereas *Sptlc1* gene expression was comparable between CRE$^-$ and CRE$^+$ mice on HFD (Fig. 5*B*). There was no difference in anti-inflammatory gene, *Arg1*, or in pro-inflammatory genes *iNos*, *Il1*β, or *Tnf*α (Fig. 5*C*). Taken together, these data indicate that myeloid cell-specific *Sptlc2* is not required for HFD-induced adipose tissue inflammation. To ask whether other pathways to generate ceramide are compensating for the loss of *Sptlc2*, we examined gene expression of ceramide synthases (CerS) and sphingomyelinases in isolated adipose tissue

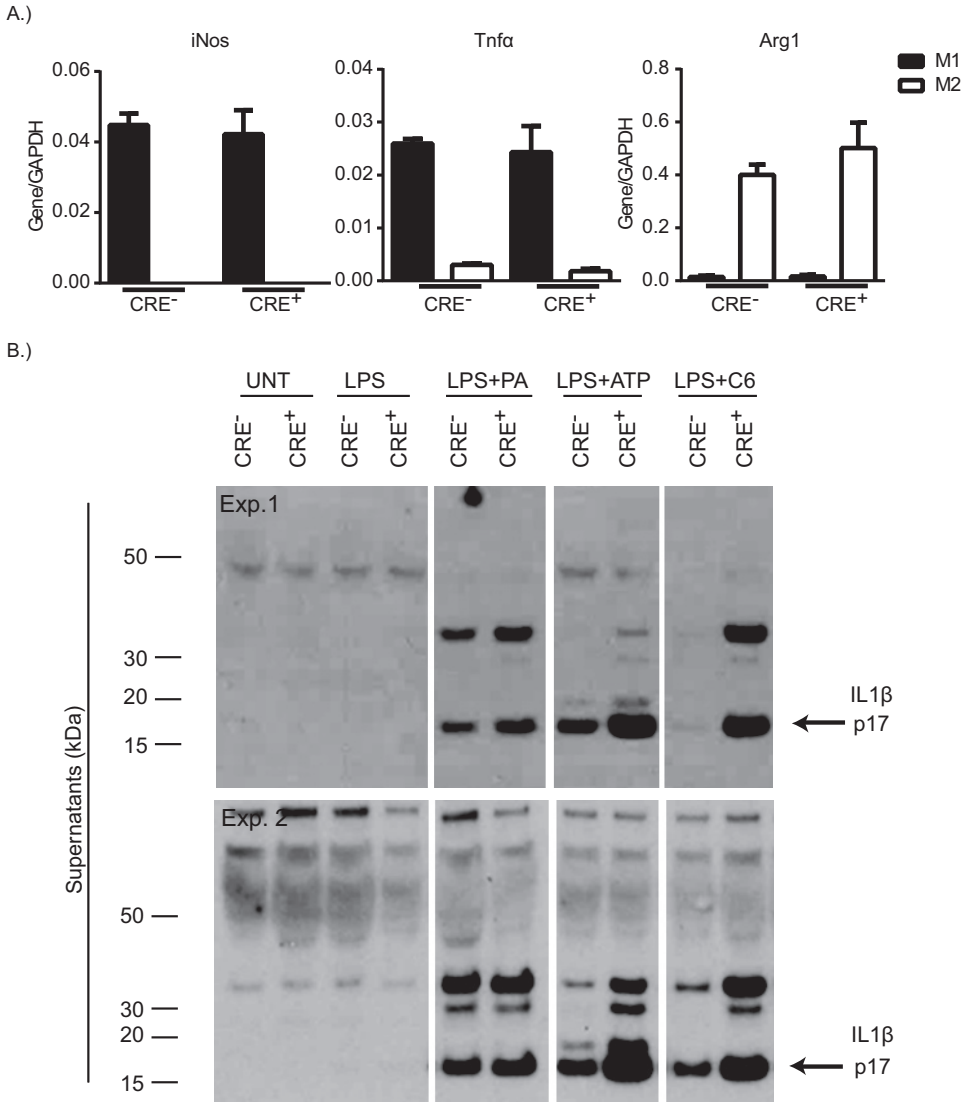

FIGURE 3. **Sptlc2 is not required for macrophage polarization or inflammasome activation *in vitro*.** *A*, *iNos*, *Tnfα*, or *arg1* gene expression, normalized to *gapdh*, from CRE^- or CRE^+ BMDMs that have been polarized to M1 (*filled bars*) or M2 (*open bars*). *B*, two Western blots from individual experiments of IL1β protein in supernatants of CRE^- or CRE^+ BMDMs following no treatment, treatment with LPS alone, LPS plus palmitate, LPS plus ATP, or LPS plus C6 ($n = 2$–3 individual experiments). The *error bars* represent means ± S.E. *Exp.*, experiment.

macrophages. The expression levels of *CerS6*, *CerS5*, *Nsmaf*, and *Smpd1* were not altered by myeloid deficiency of *Sptlc2* (Fig. 5*D*).

Macrophage Sptlc2 Deficiency Does Not Impact HFD-induced Insulin Resistance —Myriocin treatment to block systemic *de novo* synthesis of ceramides decreases systemic sphingolipid and ceramide levels, improves insulin sensitivity, and reduces adipose tissue mass in mice on HFD (24). On a LFD, CRE^- and CRE^+ mice have comparable baseline glucose and ability to clear glucose following intraperitoneal injection of glucose (Fig. 6*A*). We examined whether myeloid-specific *de novo* synthesis of ceramides is responsible for HFD-induced decreases in insulin sensitivity using hyperinsulinemic-euglycemic clamp studies. There was no difference in glucose infusion rate between CRE^- and CRE^+ mice on HFD (Fig. 6*B*). Furthermore, whole body glucose uptake and endogenous glucose production at basal or following clamp was comparable between HFD-fed mice (Fig. 4, *C* and *D*). These data suggest that myeloid cell-specific *Sptlc2* is not required for systemic insulin sensitivity. In addition, clamp was equally able to decrease nonesterified fatty acids in CRE^- and CRE^+ HFD-fed mice (Fig. 6*E*). In agreement with this data, an insulin tolerance test in CRE^- and CRE^+ on HFD revealed similar baseline glucose and similar ability to restore glucose levels following insulin challenge (Fig. 6, *F* and *G*).

Discussion

DIO is characterized as a state of chronic, low grade inflammation with lipid and glucose alterations mediated in part by macrophage infiltration of adipose tissue (41). Palmitate induces Nlrp3 inflammasome activation and subsequent IL1β secretion during DIO; however, the mechanism for activation has not been fully elucidated (15). We have hypothesized that Nlrp3 inflammasome activation requires saturated fatty acid entry into the nonoxidative pathway and *de novo* generation of ceramide via *Sptlc2*. In these experiments, we have shown that

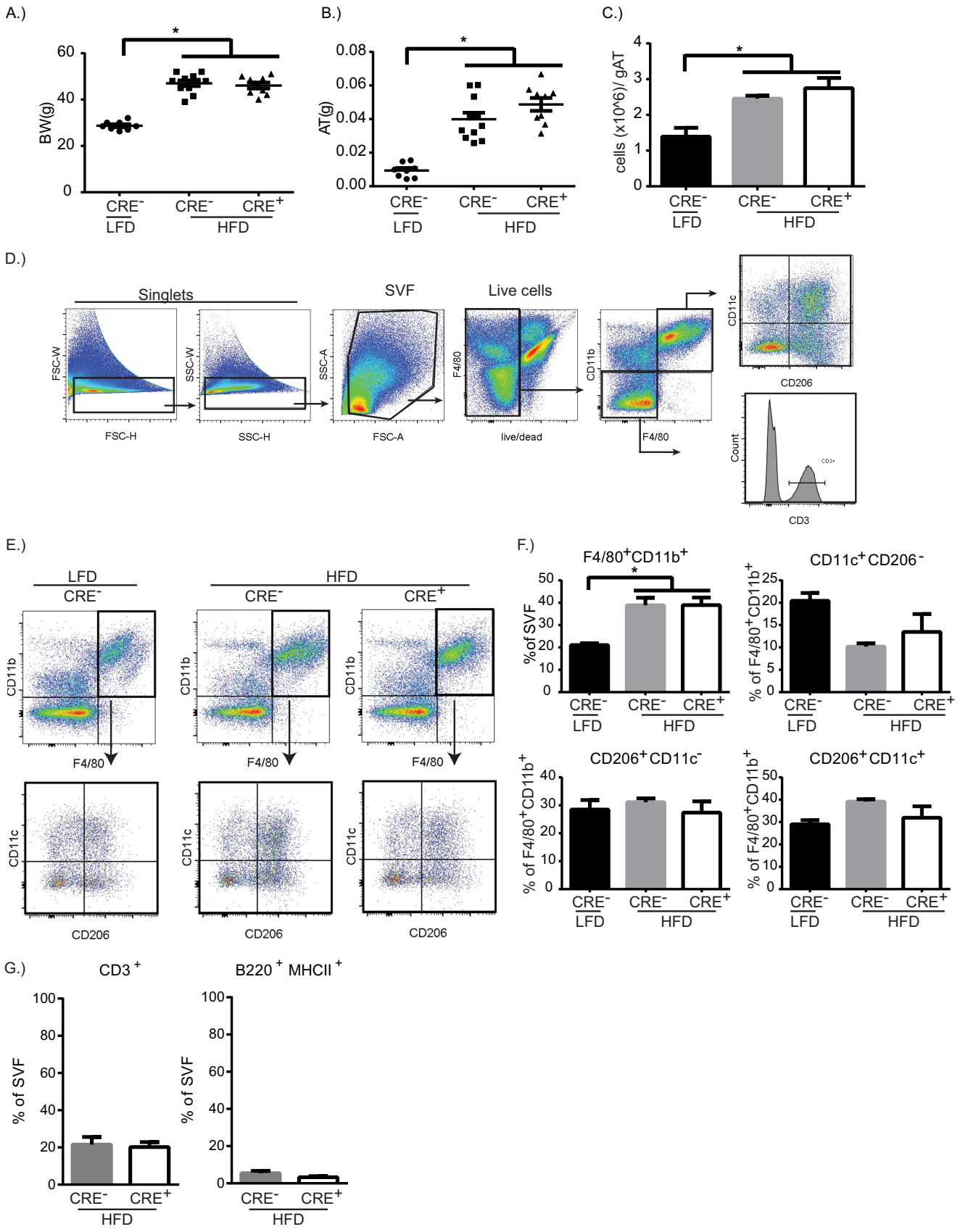
A.)
BW(g)
CRE- LFD
CRE- HFD
CRE+ HFD
B.)
AT(g)
C.)
cells (x10^6)/ gAT
D.)
Singlets
SVF
Live cells
FSC-W
FSC-H
SSC-W
SSC-H
SSC-A
FSC-A
F4/80
live/dead
CD11b
CD11c
CD206
Count
CD3
E.)
LFD
HFD
CRE-
CRE+
F.)
F4/80+CD11b+
% of SVF
CD11c+CD206-
% of F4/80+CD11b+
CD206+CD11c-
CD206+CD11c+
G.)
CD3 +
B220 + MHCII +

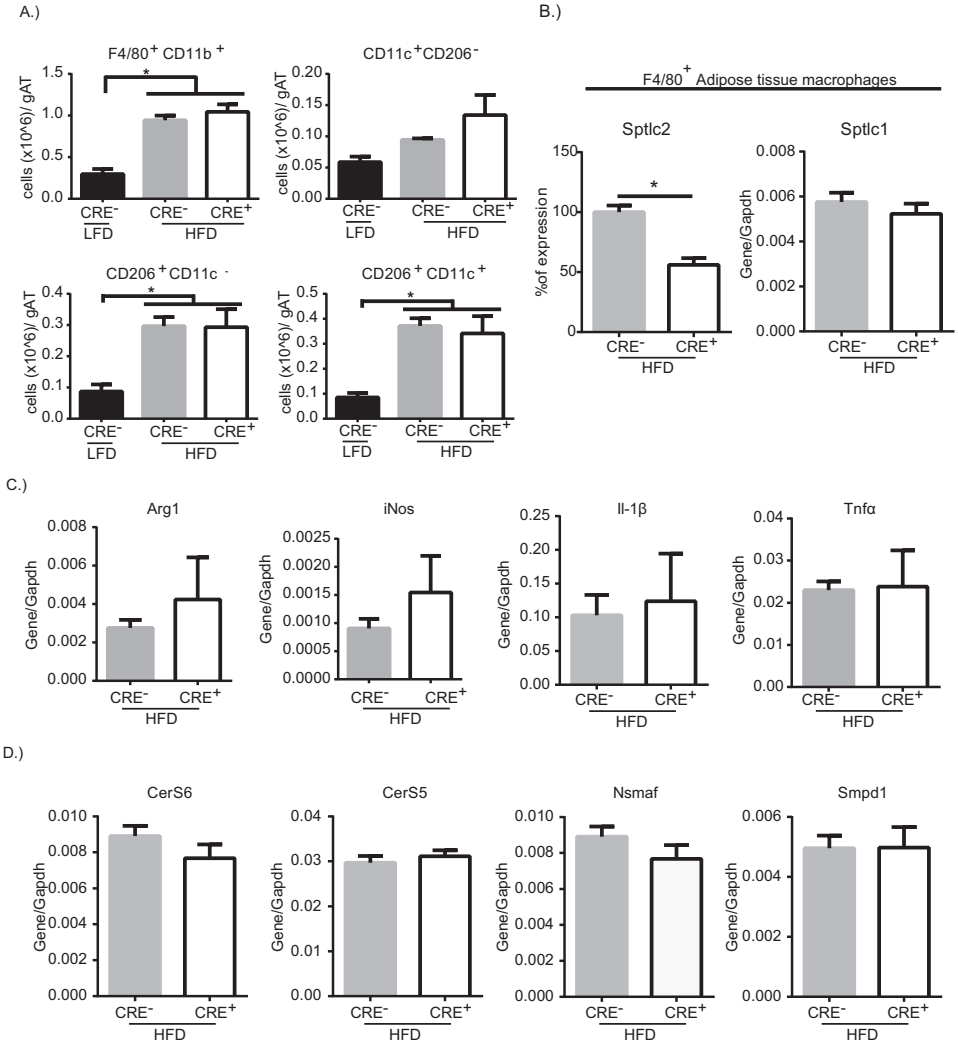

FIGURE 5. **Sptlc2-deficient adipose tissue macrophages maintain HFD-induced inflammation.** *A*, quantification of the cells/g AT for macrophages and the macrophage subpopulations from the visceral adipose tissue of CRE^- or CRE^+ mice on HFD. *B*, expression level of *Sptlc2* or *Sptlc1* in isolated $F4/80^+$ adipose tissue macrophages from CRE^- or CRE^+ mice on HFD. *C* and *D*, gene expression of *arg1*, *iNos*, and *Il1β Tnfα* (*C*) and *CerS6*, *CerS5*, *Nsmaf*, and *Smpd1* (*D*) (normalized to *Gapdh*) in isolated adipose tissue macrophages ($n = 9–10$ biological replicates; one-way ANOVA or *t* test as appropriate). *, $p < 0.05$. The *error bars* represent means ± S.E. *gAT*, gram of adipose tissue.

myeloid cell-specific deletion of *Sptlc2* is not required for inflammasome-induced adipose tissue inflammation and insulin resistance. *In vitro*, *Sptlc2* deficiency does not alter macrophage polarization or palmitate-induced IL1β secretion by the Nlrp3 inflammasome. In a model of saturated fat-induced inflammation, adipose tissue macrophage numbers, polarization, and gene expression are comparable in control mice and mice lacking myeloid cell expression of *Sptlc2*. Taken together, these data indicate that myeloid cell expression of *Sptlc2* is dispensable for inflammasome-induced adipose tissue inflammation and insulin resistance.

In vitro work using *Sptlc2*$^{-/+}$ BMDMs have shown that *Sptlc2* is required for LPS or palmitate-induced inflammatory cytokine production (40). Furthermore, *in vivo* investigations have shown that macrophage-specific *Sptlc2* promotes atherosclerotic lesions (40), highlighting the importance of ceramide synthesis in macrophages in metabolic diseases. A number of sphingolipids, downstream of ceramide synthesis, including plasminogen activator inhibitor-1, sphingosine-1-phosphate, and ceramide-1-phasphate, have been identified as possible mediators in driving metabolic-induced inflammation (17, 43, 44). These data suggested that macrophage *de novo* synthesis of ceramide was critical in regulating macrophage-driven inflammation in metabolic diseases. Here, we show that myeloid cell-specific deletion of *Sptlc2*, as shown by 75% knockdown of gene expression and complete deletion of the protein, has no altera-

FIGURE 4. **Myeloid cell-specific *Sptlc2* is not required for diet-induced inflammation.** *A–C*, Body weight (*BW*, *A*), visceral adipose tissue weight (*AT*, *B*), and cells per gram of adipose tissue (*gAT*, *C*) after 13 weeks of LFD or HFD in CRE^- or CRE^+ mice. *D*, gating strategy to analyze stromavascular fraction (*SVF*) of adipose tissue. *E*, representative dot plots of $F4/80^+CD11b^+$ cells from adipose tissue of CRE^- mice on LFD, CRE^- mice on HFD, or CRE^+ mice on HFD. $F4/80^+CD11b^+$ cells were gated on to analyze CD206 and CD11c expression. *F*, quantification of the percentage of macrophage and the macrophage subpopulations. *G*, quantification of the percentage of lymphocytes, $CD3^+$ T cells, and $B220^+$ B cells, in adipose tissue from HFD-mice ($n = 9–10$ biological replicates; one-way ANOVA or *t* test as appropriate). *, $p < 0.05$. The *error bars* represent means ± S.E.

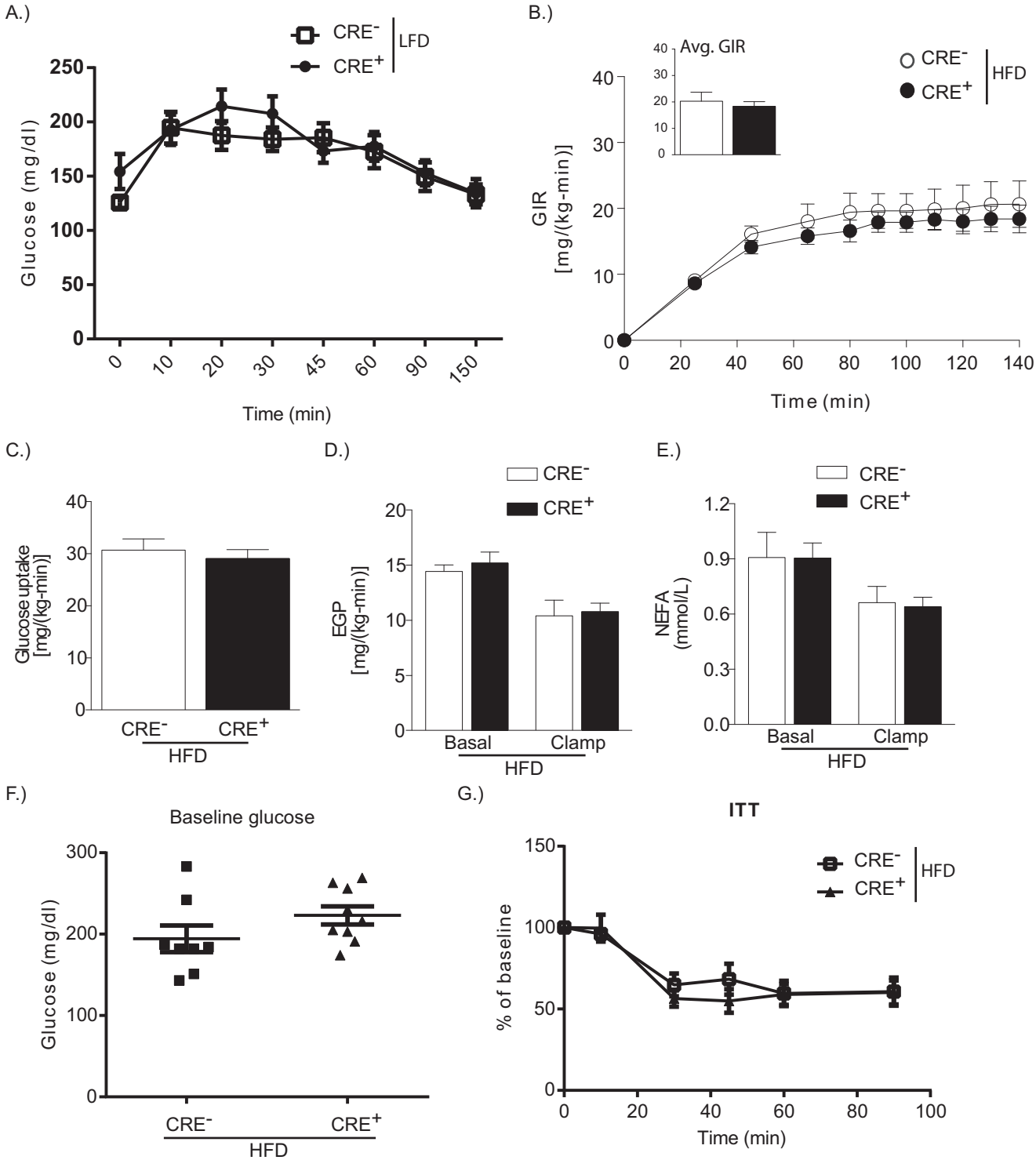

FIGURE 6. **Macrophage-specific *Sptlc2* is not required for diet-induced insulin resistance.** *A*, glucose tolerance test on LFD-fed CRE$^-$ or CRE$^+$ mice. *B*, glucose infusion rates (*GIR*) during hyperinsulinemic-euglycemic clamps in CRE$^-$ or CRE$^+$ mice on HFD for 12 weeks. The *inset* shows the average glucose infusion rate (*Avg. GIR*). *C*, whole body glucose uptake. *D*, endogenous glucose production (*EGP*) at basal and after clamp. *E*, nonesterified fatty acid level in the blood at basal and after clamp ($n = 4$ CRE$^-$; $n = 7$ CRE$^+$). *F* and *G*, baseline glucose levels after a 4-h fast (*F*) and at time points after intraperitoneal injection of insulin (*G*) (insulin tolerance test, *ITT*) in CRE$^-$ or CRE$^+$ mice on HFD ($n = 8$; *t* test). *, $p < 0.05$. The *error bars* represent means ± S.E.

tion on macrophage response *in vitro* to a single stimulus or in a mouse model of DIO. Our data, although unexpected, help to portray a more complete picture of fatty acid fate in macrophages and eliminate mechanisms that are responsible for ceramide generation as therapeutic targets of certain metabolic complications.

Furthermore, a number of publications have identified that myriocin, an SPT-specific inhibitor, promotes remarkable reductions in DIO-induced symptoms, including reduced ceramide accumulation, reduced adipose tissue, smaller adipocytes, improved insulin signaling through Akt, and improved metabolic function (21, 24, 25). The differences between these

and our data are likely due to the ability of myriocin to inhibit whole body ceramide synthesis. SPT is a constitutive enzyme with activities in regulating cellular sphingolipids in all cell types; its inhibition alters total cellular sphingolipids, and these alterations are likely to be beneficial to cells with lipid dysregulation but damaging to cells that lack exposure to excess palmitate and ceramide synthesis. Tissue-specific or cell-specific inhibition of ceramide synthesis during lipid dysregulation, for example in the liver or muscle, is an attractive prospect for reducing inflammation and improving insulin sensitivity. In agreement with this concept, overexpression of acid ceramidase in liver or adipocytes improves systemic insulin sensitivity, hepatic lipid accumulation, and adipose tissue inflammation (23). It remains to be studied whether elevation of ceramide degradation enzymes in macrophages will lower the "lipotoxic DAMP load" that causes inflammasome activation in obesity.

Sptlc2 is the rate-limiting subunit of the SPT enzyme and is required for the *de novo* synthesis of ceramide; however, other mechanisms for generating ceramide include the hydrolysis of sphingomyelin (salvage pathway) or synthesis from sphingosine and more complex sphingolipids (recycling pathway) (20, 45). Degradation of sphingomyelin requires sphingomyelinases, whereas ceramide synthases catalyze the recycling of sphingolipids, as part of a carefully regulated process for meeting the cellular demands of lipids (20). Our data shows that there is no change in gene expression of these ceramide synthases or of sphingomyelinases in adipose tissue macrophages because of deletion of *Sptlc2*. This suggests that other pathways for generating ceramides (salvage, recycling pathways) are not up-regulated in compensation for loss of the *de novo* pathway. Recent publications are in agreement with our data, suggesting that ceramide synthesis in myeloid cells is not critical for diet-induced inflammation. Deletion of CerS6, which is up-regulated in the white adipose tissue of high fat-fed mice, in macrophages failed to prevent diet-induced adipose tissue inflammation or insulin resistance (46). In our experiments, adipose tissue macrophages highly express both *CerS5* and *CerS6*. Taken together, these data indicate that ceramide synthesis in macrophages is dispensable when targeting DIO-induced inflammation and metabolic disorders. Given that ceramides are also present with the cell membranes, macrophages may accumulate ceramide via cellular membrane degradation following phagocytosis of dead or dying cells.

Macrophages are present in the lean state and are critical in promoting diet-induced adipose tissue inflammation. $CD11c^+$ macrophages infiltrate the adipose tissue, surround necrotic adipocytes, and release inflammatory cytokines (10). Not only are macrophages directly exposed to fatty acids released from dying adipocytes, but systemically, diet-induced increased serum fatty acids cause chronic exposure to macrophages. Macrophages express fatty acid receptors, including CD36, which when deleted, prevents diet-induced adipose tissue inflammation (47), indicating that macrophage uptake of fatty acids mediates HFD-induced inflammation. Upon lipid uptake, fatty acids can be stored as triglyceride in lipid droplets and enter into an oxidative pathway for metabolism to ATP or a nonoxidative pathway for conversion into cell-required sphingolipids or signaling molecules (20). The fate of fatty acids following release from dying adipocytes is unclear, although a recent study has shown the importance of lysosomal biogenesis and metabolism of lipids in adipose tissue macrophages following DIO (9), suggesting that a portion may be metabolized. Other investigations have underscored the importance of the type of fatty acids in eliciting inflammation, because omega-3 supplementation is sufficient to reduce HFD-induced adipose tissue inflammation (48). In this publication, we have eliminated the possibility that palmitate entry into the nonoxidative pathway causes Nlrp3 inflammasome-driven inflammation. These data suggest that the metabolic fate of palmitate could be at least partly independent from its ability to induce inflammation; alternatively storage as triglycerides is a potential mechanism for inflammation.

Macrophages are tissue resident cells that are critical for maintaining homeostasis through immunometabolic interactions. Saturated fatty acid is a metabolite capable of eliciting Nlrp3 inflammasome activation and promoting dysregulated glucose metabolism (13). Its mechanism of action is known to involve AMPK inhibition and ROS, but whether its metabolism is required for activation is still incompletely understood. Therapeutic attempts at improving metabolic dysfunction have been mostly unsuccessful; narrowing the number of viable translatable approaches to improve metabolic syndrome is critical in type 2 diabetes and human obesity. We have used *in vitro* and *in vivo* mouse models to eliminate the *de novo* ceramide synthesis as a potential mechanism and allow future research to focus on other significant pathways of ceramide homeostasis or degradation in macrophages.

Author Contributions—C. D. C. participated in the design of the study, coordinated and carried out experiments, performed the analysis, and wrote the manuscript. K. Y. N. participated in study design and assisted with experiments and manuscript edits. M. J. J. performed the experiments and analysis shown in Fig. 6. G. I. S. participated in experimental design and edits of the manuscript. B. E. C. and G. S. S. assisted with experimental design and data analysis and provided MCAT mice for experiments. V. D. D. conceived and coordinated the study and participated in the writing of the manuscript. All authors reviewed the results and approved the final version of the manuscript.

Acknowledgment—We thank Dr. Xian-Cheng Jiang for generating and making available Sptlc2-floxed mice.

Note Added in Proof—Brooke E. Christian's contributions to this article fulfill the JBC authorship criteria, but her authorship was inadvertently omitted from the version of the article that was published on October 5, 2015, as a Paper in Press.

References

1. Hossain, P., Kawar, B., and El Nahas, M. (2007) Obesity and diabetes in the developing world: a growing challenge. *N. Engl. J. Med.* **356,** 213–215
2. Gregor, M. F., and Hotamisligil, G. S. (2011) Inflammatory mechanisms in obesity. *Annu. Rev. Immunol.* **29,** 415–445
3. McNelis, J. C., and Olefsky, J. M. (2014) Macrophages, immunity, and metabolic disease. *Immunity* **41,** 36–48
4. Lumeng, C. N., and Saltiel, A. R. (2011) Inflammatory links between obesity and metabolic disease. *J. Clin. Invest.* **121,** 2111–2117
5. Nishimura, S., Manabe, I., Nagasaki, M., Eto, K., Yamashita, H., Ohsugi,

M., Otsu, M., Hara, K., Ueki, K., Sugiura, S., Yoshimura, K., Kadowaki, T., and Nagai, R. (2009) CD8+ effector T cells contribute to macrophage recruitment and adipose tissue inflammation in obesity. *Nat. Med.* **15,** 914–920
6. Winer, D. A., Winer, S., Shen, L., Wadia, P. P., Yantha, J., Paltser, G., Tsui, H., Wu, P., Davidson, M. G., Alonso, M. N., Leong, H. X., Glassford, A., Caimol, M., Kenkel, J. A., Tedder, T. F., McLaughlin, T., Miklos, D. B., Dosch, H. M., and Engleman, E. G. (2011) B cells promote insulin resistance through modulation of T cells and production of pathogenic IgG antibodies. *Nat. Med.* **17,** 610–617
7. Weisberg, S. P., McCann, D., Desai, M., Rosenbaum, M., Leibel, R. L., and Ferrante, A. W., Jr. (2003) Obesity is associated with macrophage accumulation in adipose tissue. *J. Clin. Invest.* **112,** 1796–1808
8. Winer, S., Chan, Y., Paltser, G., Truong, D., Tsui, H., Bahrami, J., Dorfman, R., Wang, Y., Zielenski, J., Mastronardi, F., Maezawa, Y., Drucker, D. J., Engleman, E., Winer, D., and Dosch, H. M. (2009) Normalization of obesity-associated insulin resistance through immunotherapy. *Nat. Med.* **15,** 921–929
9. Xu, X., Grijalva, A., Skowronski, A., van Eijk, M., Serlie, M. J., and Ferrante, A. W., Jr. (2013) Obesity activates a program of lysosomal-dependent lipid metabolism in adipose tissue macrophages independently of classic activation. *Cell Metab.* **18,** 816–830
10. Lumeng, C. N., DelProposto, J. B., Westcott, D. J., and Saltiel, A. R. (2008) Phenotypic switching of adipose tissue macrophages with obesity is generated by spatiotemporal differences in macrophage subtypes. *Diabetes* **57,** 3239–3246
11. Schroder, K., and Tschopp, J. (2010) The inflammasomes. *Cell* **140,** 821–832
12. Henao-Mejia, J., Elinav, E., Thaiss, C. A., and Flavell, R. A. (2014) Inflammasomes and metabolic disease. *Annu. Rev. Physiol.* **76,** 57–78
13. Vandanmagsar, B., Youm, Y. H., Ravussin, A., Galgani, J. E., Stadler, K., Mynatt, R. L., Ravussin, E., Stephens, J. M., and Dixit, V. D. (2011) The NLRP3 inflammasome instigates obesity-induced inflammation and insulin resistance. *Nat. Med.* **17,** 179–188
14. Stienstra, R., van Diepen, J. A., Tack, C. J., Zaki, M. H., van de Veerdonk, F. L., Perera, D., Neale, G. A., Hooiveld, G. J., Hijmans, A., Vroegrijk, I., van den Berg, S., Romijn, J., Rensen, P. C., Joosten, L. A., Netea, M. G., and Kanneganti, T. D. (2011) Inflammasome is a central player in the induction of obesity and insulin resistance. *Proc. Natl. Acad. Sci. U.S.A.* **108,** 15324–15329
15. Wen, H., Gris, D., Lei, Y., Jha, S., Zhang, L., Huang, M. T., Brickey, W. J., and Ting, J. P. (2011) Fatty acid-induced NLRP3-ASC inflammasome activation interferes with insulin signaling. *Nat. Immunol.* **12,** 408–415
16. Haneklaus, M., O'Neill, L. A., and Coll, R. C. (2013) Modulatory mechanisms controlling the NLRP3 inflammasome in inflammation: recent developments. *Curr. Opin. Immunol.* **25,** 40–45
17. Shah, C., Yang, G., Lee, I., Bielawski, J., Hannun, Y. A., and Samad, F. (2008) Protection from high fat diet-induced increase in ceramide in mice lacking plasminogen activator inhibitor 1. *J. Biol. Chem.* **283,** 13538–13548
18. Samad, F., Badeanlou, L., Shah, C., and Yang, G. (2011) Adipose tissue and ceramide biosynthesis in the pathogenesis of obesity. *Adv. Exp. Med. Biol.* **721,** 67–86
19. Blachnio-Zabielska, A. U., Pulka, M., Baranowski, M., Nikolajuk, A., Zabielski, P., Górska, M., and Górski, J. (2012) Ceramide metabolism is affected by obesity and diabetes in human adipose tissue. *J. Cell. Physiol.* **227,** 550–557
20. Gault, C. R., Obeid, L. M., and Hannun, Y. A. (2010) An overview of sphingolipid metabolism: from synthesis to breakdown. *Adv. Exp. Med. Biol.* **688,** 1–23
21. Holland, W. L., Brozinick, J. T., Wang, L. P., Hawkins, E. D., Sargent, K. M., Liu, Y., Narra, K., Hoehn, K. L., Knotts, T. A., Siesky, A., Nelson, D. H., Karathanasis, S. K., Fontenot, G. K., Birnbaum, M. J., and Summers, S. A. (2007) Inhibition of ceramide synthesis ameliorates glucocorticoid-, saturated-fat-, and obesity-induced insulin resistance. *Cell Metab.* **5,** 167–179
22. Bikman, B. T., and Summers, S. A. (2011) Ceramides as modulators of cellular and whole-body metabolism. *J. Clin. Invest.* **121,** 4222–4230
23. Xia, J. Y., Holland, W. L., Kusminski, C. M., Sun, K., Sharma, A. X., Pearson, M. J., Sifuentes, A. J., McDonald, J. G., Gordillo, R., and Scherer, P. E. (2015) Targeted induction of ceramide degradation leads to improved systemic metabolism and reduced hepatic steatosis. *Cell Metab.* **22,** 266–278
24. Yang, G., Badeanlou, L., Bielawski, J., Roberts, A. J., Hannun, Y. A., and Samad, F. (2009) Central role of ceramide biosynthesis in body weight regulation, energy metabolism, and the metabolic syndrome. *Am. J. Physiol. Endocrinol. Metab.* **297,** E211–E224
25. Ussher, J. R., Koves, T. R., Cadete, V. J., Zhang, L., Jaswal, J. S., Swyrd, S. J., Lopaschuk, D. G., Proctor, S. D., Keung, W., Muoio, D. M., and Lopaschuk, G. D. (2010) Inhibition of de novo ceramide synthesis reverses diet-induced insulin resistance and enhances whole-body oxygen consumption. *Diabetes* **59,** 2453–2464
26. Schilling, J. D., Machkovech, H. M., He, L., Sidhu, R., Fujiwara, H., Weber, K., Ory, D. S., and Schaffer, J. E. (2013) Palmitate and lipopolysaccharide trigger synergistic ceramide production in primary macrophages. *J. Biol. Chem.* **288,** 2923–2932
27. Li, Z., Li, Y., Chakraborty, M., Fan, Y., Bui, H. H., Peake, D. A., Kuo, M. S., Xiao, X., Cao, G., and Jiang, X. C. (2009) Liver-specific deficiency of serine palmitoyltransferase subunit 2 decreases plasma sphingomyelin and increases apolipoprotein E levels. *J. Biol. Chem.* **284,** 27010–27019
28. Schriner, S. E., Linford, N. J., Martin, G. M., Treuting, P., Ogburn, C. E., Emond, M., Coskun, P. E., Ladiges, W., Wolf, N., Van Remmen, H., Wallace, D. C., and Rabinovitch, P. S. (2005) Extension of murine life span by overexpression of catalase targeted to mitochondria. *Science* **308,** 1909–1911
29. Nolan, T., Hands, R. E., and Bustin, S. A. (2006) Quantification of mRNA using real-time RT-PCR. *Nat. Protoc.* **1,** 1559–1582
30. Ayala, J. E., Samuel, V. T., Morton, G. J., Obici, S., Croniger, C. M., Shulman, G. I., Wasserman, D. H., McGuinness, O. P., and NIH Mouse Metabolic Phenotyping Center Consortium (2010) Standard operating procedures for describing and performing metabolic tests of glucose homeostasis in mice. *Dis. Model Mech.* **3,** 525–534
31. Jurczak, M. J., Lee, A. H., Jornayvaz, F. R., Lee, H. Y., Birkenfeld, A. L., Guigni, B. A., Kahn, M., Samuel, V. T., Glimcher, L. H., and Shulman, G. I. (2012) Dissociation of inositol-requiring enzyme (IRE1alpha)-mediated c-Jun N-terminal kinase activation from hepatic insulin resistance in conditional X-box-binding protein-1 (XBP1) knock-out mice. *J. Biol. Chem.* **287,** 2558–2567
32. Youm, Y. H., Nguyen, K. Y., Grant, R. W., Goldberg, E. L., Bodogai, M., Kim, D., D'Agostino, D., Planavsky, N., Lupfer, C., Kanneganti, T. D., Kang, S., Horvath, T. L., Fahmy, T. M., Crawford, P. A., Biragyn, A., Alnemri, E., and Dixit, V. D. (2015) The ketone metabolite beta-hydroxybutyrate blocks NLRP3 inflammasome-mediated inflammatory disease. *Nat. Med.* **21,** 263–269
33. Villena, J., Henriquez, M., Torres, V., Moraga, F., Díaz-Elizondo, J., Arredondo, C., Chiong, M., Olea-Azar, C., Stutzin, A., Lavandero, S., and Quest, A. F. (2008) Ceramide-induced formation of ROS and ATP depletion trigger necrosis in lymphoid cells. *Free Radic. Biol. Med.* **44,** 1146–1160
34. Zhou, R., Yazdi, A. S., Menu, P., and Tschopp, J. (2011) A role for mitochondria in NLRP3 inflammasome activation. *Nature* **469,** 221–225
35. Lee, H. Y., Choi, C. S., Birkenfeld, A. L., Alves, T. C., Jornayvaz, F. R., Jurczak, M. J., Zhang, D., Woo, D. K., Shadel, G. S., Ladiges, W., Rabinovitch, P. S., Santos, J. H., Petersen, K. F., Samuel, V. T., and Shulman, G. I. (2010) Targeted expression of catalase to mitochondria prevents age-associated reductions in mitochondrial function and insulin resistance. *Cell Metab.* **12,** 668–674
36. Vetrano, A. M., Heck, D. E., Mariano, T. M., Mishin, V., Laskin, D. L., and Laskin, J. D. (2005) Characterization of the oxidase activity in mammalian catalase. *J. Biol. Chem.* **280,** 35372–35381
37. Muñoz-Planillo, R., Kuffa, P., Martínez-Colón, G., Smith, B. L., Rajendiran, T. M., and Núñez, G. (2013) K^+ efflux is the common trigger of NLRP3 inflammasome activation by bacterial toxins and particulate matter. *Immunity* **38,** 1142–1153
38. Petersen, K. F., Befroy, D., Dufour, S., Dziura, J., Ariyan, C., Rothman, D. L., DiPietro, L., Cline, G. W., and Shulman, G. I. (2003) Mitochondrial dysfunction in the elderly: possible role in insulin resistance. *Science* **300,**

1140–1142
39. Furukawa, S., Fujita, T., Shimabukuro, M., Iwaki, M., Yamada, Y., Nakajima, Y., Nakayama, O., Makishima, M., Matsuda, M., and Shimomura, I. (2004) Increased oxidative stress in obesity and its impact on metabolic syndrome. *J. Clin. Invest.* **114,** 1752–1761
40. Chakraborty, M., Lou, C., Huan, C., Kuo, M. S., Park, T. S., Cao, G., and Jiang, X. C. (2013) Myeloid cell-specific serine palmitoyltransferase subunit 2 haploinsufficiency reduces murine atherosclerosis. *J. Clin. Invest.* **123,** 1784–1797
41. Chawla, A., Nguyen, K. D., and Goh, Y. P. (2011) Macrophage-mediated inflammation in metabolic disease. *Nat. Rev. Immunol.* **11,** 738–749
42. Winer, D. A., Winer, S., Chng, M. H., Shen, L., and Engleman, E. G. (2014) B Lymphocytes in obesity-related adipose tissue inflammation and insulin resistance. *Cell. Mol. Life Sci.* **71,** 1033–1043
43. Mitsutake, S., Date, T., Yokota, H., Sugiura, M., Kohama, T., and Igarashi, Y. (2012) Ceramide kinase deficiency improves diet-induced obesity and insulin resistance. *FEBS Lett.* **586,** 1300–1305
44. Wang, J., Badeanlou, L., Bielawski, J., Ciaraldi, T. P., and Samad, F. (2014) Sphingosine kinase 1 regulates adipose proinflammatory responses and insulin resistance. *Am. J. Physiol. Endocrinol. Metab.* **306,** E756–E768
45. Xia, J. Y., Morley, T. S., and Scherer, P. E. (2014) The adipokine/ceramide axis: key aspects of insulin sensitization. *Biochimie* **96,** 130–139
46. Turpin, S. M., Nicholls, H. T., Willmes, D. M., Mourier, A., Brodesser, S., Wunderlich, C. M., Mauer, J., Xu, E., Hammerschmidt, P., Brönneke, H. S., Trifunovic, A., LoSasso, G., Wunderlich, F. T., Kornfeld, J. W., Blüher, M., Krönke, M., and Brüning, J. C. (2014) Obesity-induced CerS6-dependent C16:0 ceramide production promotes weight gain and glucose intolerance. *Cell Metab.* **20,** 678–686
47. Nicholls, H. T., Kowalski, G., Kennedy, D. J., Risis, S., Zaffino, L. A., Watson, N., Kanellakis, P., Watt, M. J., Bobik, A., Bonen, A., Febbraio, M., Lancaster, G. I., and Febbraio, M. A. (2011) Hematopoietic cell-restricted deletion of CD36 reduces high-fat diet-induced macrophage infiltration and improves insulin signaling in adipose tissue. *Diabetes* **60,** 1100–1110
48. Yan, Y., Jiang, W., Spinetti, T., Tardivel, A., Castillo, R., Bourquin, C., Guarda, G., Tian, Z., Tschopp, J., and Zhou, R. (2013) Omega-3 fatty acids prevent inflammation and metabolic disorder through inhibition of NLRP3 inflammasome activation. *Immunity* **38,** 1154–1163